Determination of Cake Properties in Ultrafiltration of Nano-colloids Based on Single Step-up Pressure Filtration Test

Eiji Iritani, Nobuyuki Katagiri, and Masatoshi Tsukamoto
Dept. of Chemical Engineering, Nagoya University, Furo-cho, Chikusa-ku, Nagoya 464-8603, Japan

Kuo-Jen Hwang
Dept. of Chemical and Materials Engineering, Tamkang University, 151, Yingzhuan Rd., Tamsui, New Taipei City 25137, Taiwan

DOI 10.1002/aic.14262
Published online November 18, 2013 in Wiley Online Library (wileyonlinelibrary.com)

The single step-up pressure filtration test was developed to determine the pressure dependence of average specific resistance of the cake formed in ultrafiltration of a variety of nano-colloids over a wide range of pressure drops across the cake. The values of the average specific resistance at extremely low pressures were obtained from only the flux decline data through the use of the distinct time variation of the pressure drop across the cake generated by using the ultrafiltration membrane with a high hydraulic resistance under the low filtration pressure in the first step of filtration. The values at higher pressures were obtained from the time variation of the filtration rate induced by a stepwise increase in the pressure. The correlations between the average specific cake resistance and the pressure drop across the cake were evaluated using only the flux decline data for a variety of different proteins and nanoparticles. © 2013 American Institute of Chemical Engineers *AIChE J*, 60: 289–299, 2014
Keywords: ultrafiltration, cake filtration, single step-up pressure filtration, specific cake resistance, nano-colloid

Introduction

Ultrafiltration of nano-colloids such as protein solutions and nano particulate suspensions has become increasingly important in widely diversified fields of nanotechnology, biotechnology, biomedicine, and the dairy and food industry. It is generally recognized that one of the major bottlenecks in more widespread use of ultrafiltration systems is a dramatic flux decline known as membrane fouling. One factor of such flux decline is attributed to the formation of highly resistant filter cake caused by accumulation of nanoparticles or macromolecules on the membrane surface during ultrafiltration.[1–4] Therefore, the accurate and expeditious determination of the properties of the filter cake deposited on the membrane surface during ultrafiltration based on simple and precise laboratory tests is a key factor in the design of new ultrafilter equipment and optimization of commercial ultrafiltration operations.

In the conventional cake filtration carried out using a coarse filter medium (coarse such as a filter cloth or filter paper compared to the membrane), several laboratory filtration tests using an unstirred dead-end filter have been so far developed based on the existing compressible cake filtration theory.[5–7] Above all, constant pressure filtration tests are the method most commonly employed in industrial laboratories because of the ease of the testing method, but a set of tests has to be conducted with varying filtration pressure in order to evaluate the relation between the average specific cake resistance α_{av} and the applied filtration pressure p, resulting in the evaluation of the cake compressibility. Constant rate filtration tests are more significant for finding the compressibility factor of the filter cake from only one test, but it is necessary to measure the time variation of not only the filtrate volume but also the filtration pressure.

Tiller et al.[8] originally proposed the revised filtration theory in which α_{av} varied during the course of filtration even under constant pressure conditions since the pressure drop Δp_c across the filter cake increased with time.[9,10] Vorobiev[11] presented the revised filtration theory applicable also to the compressible filter medium. Teo et al.[12] developed a method for evaluating α_{av} from the instantaneous filtration rate in constant pressure filtration by making use of the variation with time of the pressure drop Δp_c across the cake calculated from the flux decline data.

In previous articles,[13,14] the single constant pressure filtration test was developed to employ a filter medium with a high hydraulic resistance compared to the resistance of the filter cake, resulting in the observable time variation of Δp_c. As a result, the pressure dependence of α_{av} in cake filtration of particulate suspension was evaluated over a wide range of Δp_c from only one test. However, the single constant pressure filtration test conducted at a high filtration pressure has difficulty obtaining the pressure dependence of α_{av} in the range of relatively low Δp_c. Conversely, the pressure dependence of α_{av} in the range of high Δp_c cannot be evaluated from the single constant pressure filtration test conducted at a relatively low filtration pressure.

Correspondence concerning this article should be addressed to E. Iritani at iritani@nuce.nagoya-u.ac.jp.

The step-up pressure filtration test in which p is increased in stages in the course of filtration was developed as an alternative test procedure for determining α_{av} as a function of Δp_c in cake filtration of particulate suspension.[15,16] When the appropriate values of the step-up pressure is selected, the method provides the pressure dependence of α_{av} in the wide pressure range that is inaccessible by other techniques.

In this study, a potential method is explored for simply and accurately determining the properties of the filter cake formed on the membrane surface during unstirred dead-end ultrafiltration of nano-colloids such as protein solutions and nanoparticulate suspensions. The method consists of a combination of the single constant pressure filtration test using the membrane with a high hydraulic resistance and the step-up pressure filtration test, making it possible to evaluate quantitative data on the pressure dependence of α_{av} over wider range of pressures. The filtration test is conducted using an unstirred dead-end filter initially at a relatively low filtration pressure by employing a membrane with a high hydraulic resistance compared to the resistance of the filter cake, resulting in the distinct time variation of Δp_c, and hence the pressure dependence of α_{av} is evaluated for a relatively low pressure range. Subsequently, p is increased in stages in the course of filtration in order to obtain the values of α_{av} at higher pressures. The advantage of the method is confirmed from comparisons with the existing filtration tests. The pressure dependence of α_{av} for a variety of nano-colloids such as protein solutions and nanoparticulate suspensions are compared with one another, by employing nano-colloids of bovine serum albumin (BSA), lysozyme, myoglobin, hemoglobin, γ-globulin, and silica sols comprised of nanoparticles with various sizes. In addition, the effect of pH and salt addition on α_{av} vs. Δp_c relation is elucidated for ultrafiltration of the protein solution, for instance, BSA solution.

Theory

In cake filtration, at the instant that filtration is started, the entire pressure drop is across the filter medium and the applied filtration pressure p equals the liquid pressure drop p_m across the filter medium. As the filter cake grows with time in constant pressure filtration, p_m falls and the effective pressure drop ($p - p_m$) ($= \Delta p_c$) across the filter cake builds up because of the increase in the hydraulic resistance of the growing filter cake.

A filter medium is generally selected to give a minimum resistance consistent with the filtrate production of satisfactory clarity. In this case, p_m rapidly drops to low values, and thus the filter cake absorbs most of the pressure drop over an entire period of filtration. However, if constant pressure filtration is conducted with considerably large values of the filter medium resistance, Δp_c gradually increases from zero at the start of filtration toward the value of p. Consequently, despite filtration being carried out under a constant pressure condition, variable-pressure and variable-rate filtration, where neither Δp_c nor the filtration rate u_1 is maintained constant, is actually achieved. As a result, the pressure dependence of α_{av} is easily available from only the flux decline data without monitoring the time variation of Δp_c, as mentioned later.

In the single step-up pressure filtration test developed in this study, filtration is started at the relatively low filtration pressure p_1 in the first stage of filtration by employing the ultrafiltration membrane with a high hydraulic resistance compared to the resistance of the filter cake, resulting in the visible time variations of Δp_c, as schematically shown in Figure 1. Consequently, the pressure dependence of α_{av} can be evaluated for extremely low-pressure range. Subsequently, the stepwise increase in p is conducted in the method in order to obtain α_{av} at higher Δp_c, as shown in the figure.

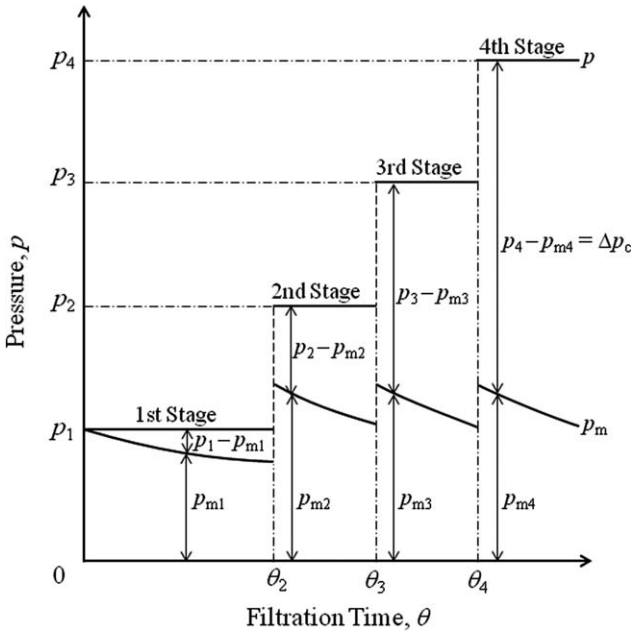

Figure 1. Pattern diagram describing principle of single step-up pressure filtration test.

In the single step-up pressure filtration test, the filtration pressure p is increased in stages in the order of p_1, p_2, p_3, and p_4 ($p_1 < p_2 < p_3 < p_4$) in the course of filtration. As filtration proceeds to the next stage, the pressure drop Δp_c across the cake profoundly increases mainly due to the increase in p, resulting in the cake compression. Consequently, filtration data is available from the method developed in this article over a wide range of Δp_c.

The method for obtaining the relation between α_{av} and Δp_c developed in this article depends on several assumptions which are summarized as follows:

1. The flow rate is constant across the cake at any instant.
2. All particles convected toward the membrane accumulate in the cake.
3. Ultimate values of porosity corresponding to the compressive pressure are attained instantaneously.
4. Colloids are dilute.
5. The pore clogging and compressibility of the membrane are negligible.

In the compressible cake filtration theory,[13,17] the basic equation relating the rate of flow through compressible filter cake to the pressure gradient is described by

$$u = \frac{1}{\mu \rho_s \alpha} \cdot \frac{\partial p_L}{\partial \omega} = -\frac{1}{\mu \rho_s \alpha} \cdot \frac{\partial p_s}{\partial \omega} \tag{1}$$

where ω is the net solid volume per unit membrane area lying from the membrane up to an arbitrary position in the filter cake, u is the apparent liquid velocity relative to solids in the filter cake at distance ω from the membrane, μ is the viscosity of the filtrate, ρ_s is the density of solids, α is the local specific cake resistance, p_L is the local hydraulic pressure, and p_s is the local solid compressive pressure.

Assuming that the flow rate u remains constant throughout the entire cake at any instant in filtration of dilute colloids,[18] Eq. 1 is integrated from $\omega = 0$ to ω_0 and $p_s = \Delta p_c$ to 0 to give

$$u_1 = \frac{dv}{d\theta} = \frac{\Delta p_c}{\mu \rho_s \omega_0 \alpha_{av}} \tag{2}$$

where u_1 is the filtration rate, v is the cumulative filtrate volume per unit membrane area, θ is the filtration time, ω_0 is the net solid volume of the entire cake per unit membrane area, and α_{av} is the average specific cake resistance given as[19]

$$\alpha_{av} = \frac{\Delta p_c}{\int_0^{\Delta p_c} \frac{1}{\alpha} dp_s} \tag{3}$$

Equation 3 is the defining equation for α_{av}, which is a unique function of the effective pressure drop Δp_c across the cake.

In the cake filtration model used in unstirred dead-end filtration, it is implicitly assumed that all particles convected toward the membrane accumulate in the filter cake.[3,20–22] On the basis of the material balance, it is convenient to transform Eq. 2 from ω_0 to v to give[8,12,14]

$$\frac{1}{u_1} = \frac{d\theta}{dv} = \frac{\mu \alpha_{av} \rho s}{\Delta p_c (1 - ms)} v \tag{4}$$

where s is the mass fraction of solids in colloids, and m is the ratio of the mass of wet to mass of dry cake. When the filtration pressure p_1 at the first stage of filtration is employed, p_m is written as

$$p_m = \mu R_m u_1 = \frac{(d\theta/dv)_m}{(d\theta/dv)} p_1 \tag{5}$$

where R_m is the hydraulic resistance provided by the membrane, and $(d\theta/dv)_m$ is the reciprocal filtration rate at the onset of filtration when no cake is present. As a result, Δp_c is represented by

$$\Delta p_c = p - p_m = p - \frac{(d\theta/dv)_m}{(d\theta/dv)} p_1 \tag{6}$$

Note that the value of p in the aforementioned equation varies in stages between p_1, p_2, p_3, and p_4 in the single step-up pressure filtration. It is important to note that the temporal variation of Δp_c can be evaluated directly from the flux decline data according to Eq. 6.

Consequently, the value of Δp_c corresponding to the value of the reciprocal filtration rate $(d\theta/dv)$ can be calculated using Eq. 6. It is assumed that ultimate values of porosity corresponding to the compressive pressure are attained instantaneously even in the single step-up pressure filtration.[15,23] Therefore, if the pressure dependence of m in Eq. 4 is known, then the employment of Eqs. 4 and 6 permits the calculation of the relation between α_{av} and Δp_c on the basis of the value of instantaneous reciprocal filtration rate $(d\theta/dv)$ for a given v-value in the single step-up pressure filtration.

Since the term $(1 - ms)$ may be approximated by unity in filtration carried out with dilute colloids, Eq. 4 reduces to

$$\frac{d\theta}{dv} = \frac{\mu \alpha_{av} \rho s}{\Delta p_c} v \tag{7}$$

In that case, the pressure dependence of α_{av} can be readily evaluated from Eqs. 6 and 7 without information about the cake dryness. In this study, this method is applied to the determination of the pressure dependence of α_{av} and the validity of the results obtained is confirmed based on comparisons with the conventional tedious methods.[5,7]

When the concentration of colloids is not dilute, the use of Eq. 7 overestimates the value of α_{av}. In that case, Eq. 4 must be used in order to obtain the accurate pressure dependence of α_{av}, and it is necessary to know the pressure dependence of m in advance. Although it is assumed that ultimate values of porosity corresponding to the compressive pressure are attained instantaneously, it is considered that, in fact, equilibrium porosities are not reached immediately with changes in pressure. Thus, it is to be noted that the data obtained right after the applied pressure increase underestimate the value of α_{av}. This method implicitly assumes that the hydraulic resistance of the membrane itself is essentially unaffected by ultrafiltration process and that the pore clogging of the membrane is considered negligible. This assumption should be valid in cases where the membranes are fully retentive to particles and solutes and the filter cake readily forms on the surface of the membrane. It is assumed that compression of the membrane is negligible in the method. When the membrane compressibility is relatively large, the analysis presented by Vorobiev[11] is available with the aid of the data of membrane compressibility, and it will be interesting to discuss the influence of membrane compressibility on the filtration data as the future issue. Therefore, it is of importance in selecting a membrane and operation that these phenomena are kept to a minimum.

According to the compressible cake filtration theory, it is apparent that the value of α_{av} substantially depends on Δp_c. As is obvious from Eq. 3, it is necessary to relate α_{av} to Δp_c in evaluating the flux decline behaviors in the filtration process. In general, it is possible to empirically represent α_{av} by the power function of Δp_c for particulate suspension as follows[24]

$$\alpha_{av} = \alpha_1 \Delta p_c^{\,n_1} \tag{8}$$

where α_1 and n_1 are the empirical constants, and a power law exponent n_1 is termed the compressibility coefficient, reflecting the degree of compressibility of the filter cake. Note that Eq. 8 holds for the effective pressure drops above some low-pressure p_i. Below the pressure p_i, the local specific cake resistance α in Eq. 3 is assumed constant although virtually no data are so far available for such low pressures.[25]

In order to describe the specific resistance for low pressures more accurately, Tiller and Lew[26] proposed an empirical equation relating α to the local solid compressive pressure p_s for particulate suspension as follows

$$\alpha = a_0 \left(1 + \frac{p_s}{p_{a1}}\right)^{n_2} \tag{9}$$

where a_0, p_{a1}, and n_2 are the empirical constants. The analytical expression for α_{av} as a function of Δp_c can be derived from integration of Eq. 9 as follows[26]

$$\alpha_{av} = \frac{a_0 (1 - n_2)(\Delta p_c / p_{a1})}{(1 + \Delta p_c / p_{a1})^{1 - n_2} - 1} \tag{10}$$

Instead, a new empirical equation is proposed as[14]

$$\alpha_{av} = a_1 \left(1 + \frac{\Delta p_c}{p_{a2}}\right)^{n_3} \tag{11}$$

Table 1. Properties of Selected Proteins

Protein	Molecular Weight (kDa)	Isoelectric pH
BSA	67	5.1
Lysozyme	14.3	11.0
Myoglobin	17.8	7.0
Hemoglobin	64.5	6.8
γ-Globulin	159	5.86 − 6.70

where a_1, p_{a2}, and n_3 are the empirical constants. Based on the aforementioned equation, the relation between α and p_s becomes

$$\alpha = a_1 \frac{(1+p_s/p_{a2})^{n_3+1}}{1+(1-n_3)p_s/p_{a2}} \tag{12}$$

The applicability of these three empirical Eqs. 8, 10, and 11 to nano-colloids will be examined on the basis of the curve fitting of the pressure dependence of α_{av} determined experimentally by the method developed in this article.

In the special case where the membrane resistance R_m is assumed to be negligible compared with the cake resistance R_c, Δp_c in Eqs. 7 and 3 is approximated by p and then these equations lead to

$$\frac{d\theta}{dv} = \frac{\mu \alpha_{av} \rho s}{p} v \tag{13}$$

$$\alpha_{av} = \frac{p}{\int_0^p \frac{1}{\alpha} dp_s} \tag{14}$$

In that case, α_{av} is also kept constant as long as p is constant. Consequently, Eq. 13 clearly indicates that the plots of $d\theta/dv$ vs. v are linear at each filtration pressure in the conventional step-up pressure filtration using the membrane with negligible resistance.[15,16]

Experimental

Materials

A variety of different proteins were employed in the ultrafiltration experiments: (a) bovine serum albumin (BSA) (Fraction V, Sigma-Aldrich Japan); (b) lysozyme from chicken egg white (Sigma-Aldrich Japan); (c) myoglobin from horse heart (Sigma-Aldrich Japan); (d) hemoglobin from bovine blood (Sigma-Aldrich); and (e) γ-globulin from bovine plasma (Sigma-Aldrich). Table 1 provides a listing of the properties of the proteins selected in this study. Moreover, the solutions of silica sol (Snowtex (ST), Nissan Chemical Industries) with three different mean particle sizes were used as the nano-colloids. The particle size distributions of silica sol were measured by a dynamic light scattering (DLS) photometer (DLS-8000, Otsuka Electronics). The mean specific surface area sizes d_s of ST-XS, ST-20, and ST-ZL employed are 4.8, 13.3, and 99.7 nm, respectively.

Dilute aqueous colloids were prepared by dispersing preweighed quantities of the solutes or solutions in ultrapure, deionized water (resistivity of at least 18 MΩ·cm) prepared by purifying tap water through ultrapure water systems equipped both with Elix-UV20 and with Milli-Q Advantage for laboratory use (Millipore). In the protein solution makeup, the desired pH value was achieved by adding small aliquots of 0.1 M solutions of NaOH or HCl for most of the proteins and by using 10 mM phosphate buffer solution in the case of γ-globulin because of the problem of dissolution of protein crystals. In some experiments the ionic strength of BSA solution was adjusted by the addition of NaCl ($C_s = 200$ mol/m^3).

Experimental apparatus and technique

Figure 2 illustrates a schematic layout of the experimental setup used to perform filtration experiments. An unstirred batch filtration cell with an effective membrane area of 24.6 cm^2 was used in this research. In the single step-up pressure filtration test, the pressure was adjusted automatically by a computer-driven electronic pressure regulator by applying compressed nitrogen gas and was increased sequentially in order of 49 (= p_1), 98 (= p_2), 196 (= p_3) and 490 (= p_4) kPa. The running time at each pressure is 4, 1, 1, and 1 h, respectively. Asymmetric regenerated cellulose ultrafiltration membranes (Millipore) with a nominal molecular weight cutoff (MWCO) of 1 kDa were employed to ensure a high membrane resistance.

The filtrate was collected in a reservoir placed on an electric balance (Shimadzu) connected to a personal computer to collect and record mass vs. time data during filtration test. The weights were converted to volumes using density correlations. The filtration rate was obtained by numerical differentiation of the volume vs. time data and the reciprocal filtration rate was represented as a function of the filtrate volume per unit effective membrane area.

For comparison, the single constant pressure filtration test was conducted using the same ultrafiltration membrane with a nominal MWCO of 1 kDa and the filtration pressure was kept constant at 49 or 490 kPa.[13,14] Moreover, a series of conventional constant pressure filtration tests were performed using the asymmetric regenerated cellulose ultrafiltration membranes (Millipore) under different filtration pressure conditions of 49, 98, 196 and 490 kPa. In this instance, the appropriate nominal MWCO of the ultrafiltration membrane was selected to ensure that the resistance of the membrane is negligibly small compared to that of the filter cake for a major portion of filtration. There was never any detectable passage of dispersed phase through the ultrafiltration membrane even in this case.

Results and Discussion

Flux decline behaviors in ultrafiltration of BSA solution

Typical data of the single step-up pressure filtration test conducted with BSA solution prepared at the isoelectric point are plotted in Figure 3a as the form of the reciprocal filtration rate ($d\theta/dv$) against the filtrate volume v per unit effective membrane area. Several data points are cut out from the figure to make it easier to identify as data points obtained from the numerical calculation are too many. It should be noted that the term ($d\theta/dv$) is a measure of the total filtration resistance R_t, as described by the Darcy's law in the form[27]

$$\frac{d\theta}{dv} = \frac{\mu R_t}{p} \tag{15}$$

In the first step of step-up pressure filtration, constant pressure filtration starts at the initial pressure p_1 of 49 kPa. Since the ultrafiltration membrane with the MWCO of 1 kDa having a high membrane resistance ($R_m = 7.71 \times 10^{13}$ m^{-1}) is used, the value of the initial reciprocal filtration rate $(d\theta/dv)_m$ is not negligible (1.58×10^4 s cm^{-1}) compared to the

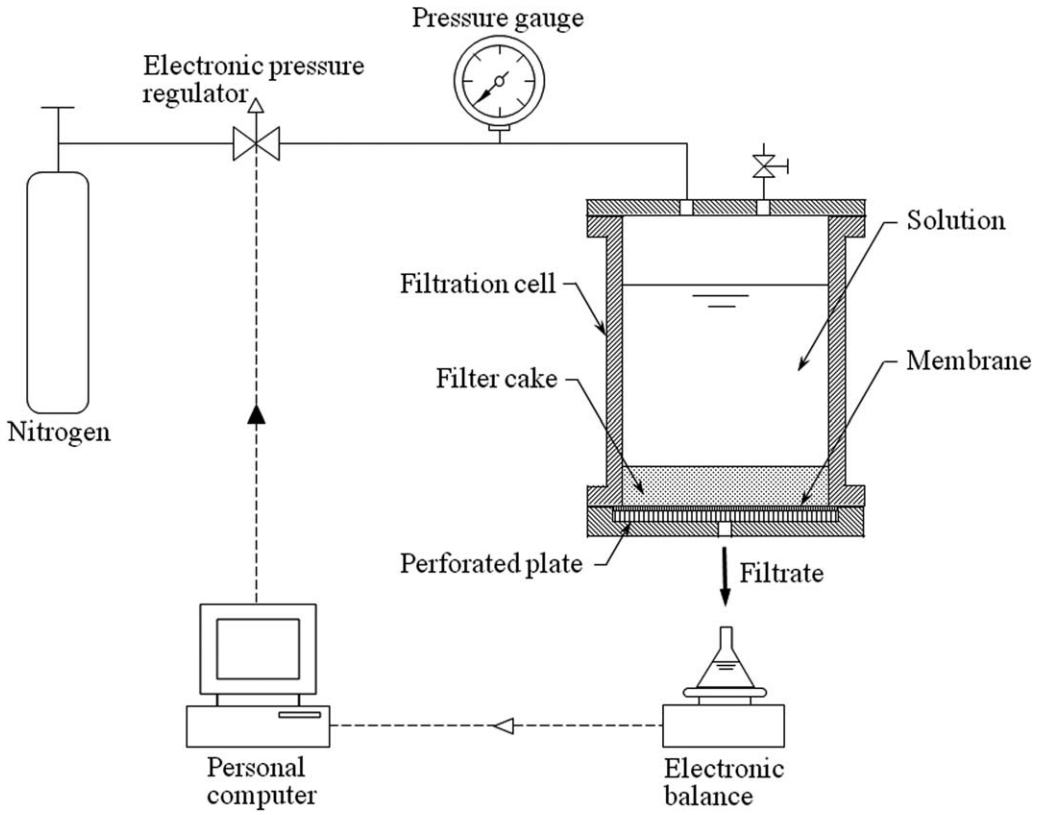

Figure 2. Schematic diagram of filtration apparatus.

subsequent variation of $d\theta/dv$, as shown in the figure. Thus, $d\theta/dv$ increases with v very gradually, and the plots exhibit the concave upward behavior. However, once the pressure suddenly increases from 49 to 98 kPa in the second step of filtration, $d\theta/dv$ decreases abruptly in response to a jump in the applied pressure leading to the increase in the driving force of filtration, but thereafter it increases with v as the filter cake grows. Subsequently, the pressure was increased to 196 and 490 kPa in stages. In either case, the trends of the transient response of the filtration rate to a step change in pressure are similar to those seen with the pressure increase to 98 kPa. The values of α_{av} for different Δp_c can be easily determined from Eqs. 6 and 7 by using the data of $d\theta/dv$ vs. v presented in Figure 3a. As seen from Eq. 15, it is instructive to convert the data of $d\theta/dv$ vs. v into a form of the total filtration resistance R_t vs. v for ease of comparison between pressures, and the results are indicated in Figure 3b. The decrease of the values associated with the step increase in the filtration pressure appearing in Figure 3a resolves in 3b, and R_t increases with increasing v, reflecting the increase in

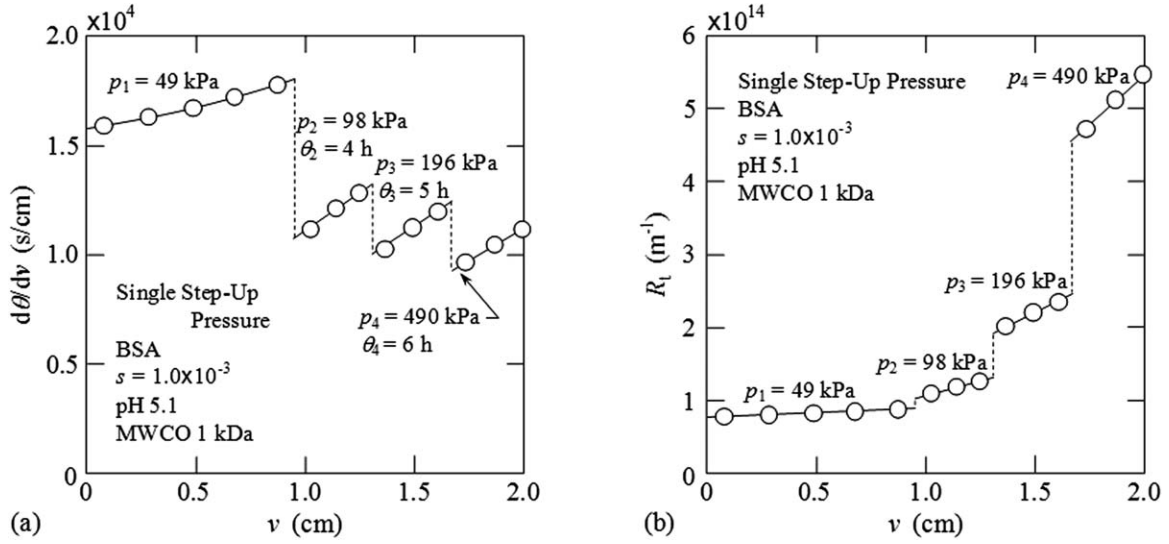

Figure 3. Flux decline behaviors in single step-up pressure filtration.

(a) Reciprocal filtration rate, and (b) total filtration resistance.

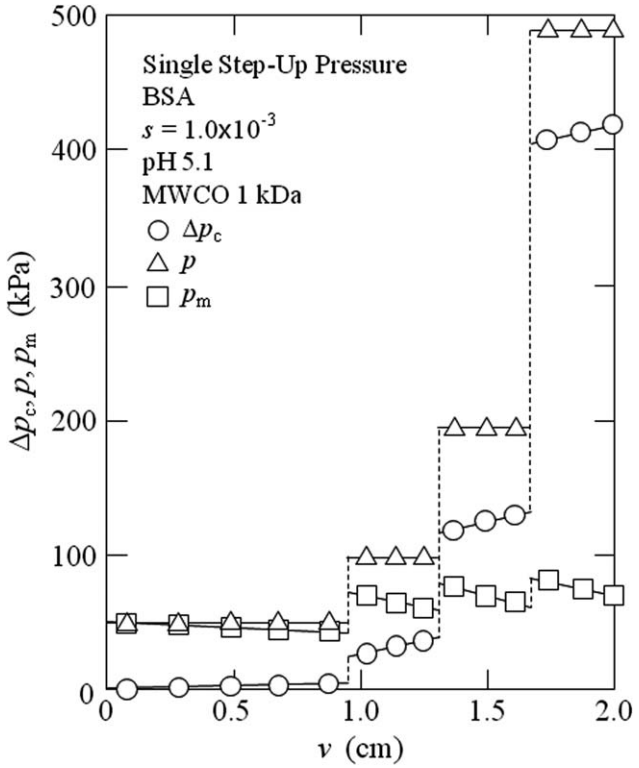

Figure 4. Variations of effective pressure drop across filter cake with filtrate volume per unit membrane area in single step-up pressure filtration.

α_{av} associated with the increase in Δp_c. In total, the plots exhibit a concave upward behavior, which is distinctive in the compressible filter cake.

Figure 4 shows the variation with v of Δp_c. Also plotted are the variation with v of p and p_m. The magnitude of p_m undergoes little change with v throughout the period of filtration. Therefore, Δp_c remarkably increases with v due to the step-up increase in p with the progress of filtration. In ultrafiltration conducted at the initial pressure of 49 kPa, Δp_c ranges from 0.42 to 5.5 kPa. In contrast, in ultrafiltration carried out at the final pressure of 490 kPa, Δp_c ranges from 410–420 kPa. Thus, Δp_c is varied over a wide range by carrying out the ultrafiltration operation with an accompanying step change in pressure using the ultrafiltration membrane with a high hydraulic resistance.

For comparison, both the single constant pressure filtration data obtained at the applied filtration pressure of 490 kPa and the conventional constant pressure filtration data obtained at the pressures of 49, 98, 196, and 490 kPa are shown in Figure 5. The plots of the single constant pressure filtration data obtained by using the membrane with a high hydraulic resistance are not linear, but exhibit a concave upward behavior, as shown in Figure 5a. Significant curvature is present only in the initial period of filtration, and thereafter $d\theta/dv$ varies almost linearly with v because the resistance of the cake becomes much higher than that of the membrane itself due to the cake growth. In contrast, the plots of the conventional constant pressure filtration data obtained by using the membrane with a negligible hydraulic resistance can be approximated by a straight line with a slope varying with the applied filtration pressure and an intercept close to zero throughout the period of filtration in accordance with Eq. 13, as shown in Figure 5b, in sharp contrast to the behaviors shown in Figures 3 and 5a. This is attributed to the negligibly small resistance of the ultrafiltration membrane with the MWCO of 10 kDa used compared to the resistance of the filter cake comprised of BSA solutes even in the incipient period of filtration. It should be noted that the gradient value of the straight line in the latter part of the plots shown in Figure 5a is almost equal to that of the straight line obtained from the pressure of 490 kPa shown in Figure 5b.

Pressure dependence of specific resistance of BSA cake

The experimental data of α_{av} are logarithmically plotted in Figure 6 against Δp_c. The open circles in Figure 6a are the result of the single step-up pressure filtration test conducted using the ultrafiltration membrane with the MWCO of 1 kDa and they are evaluated using Eqs. 6 and 7 with the data of

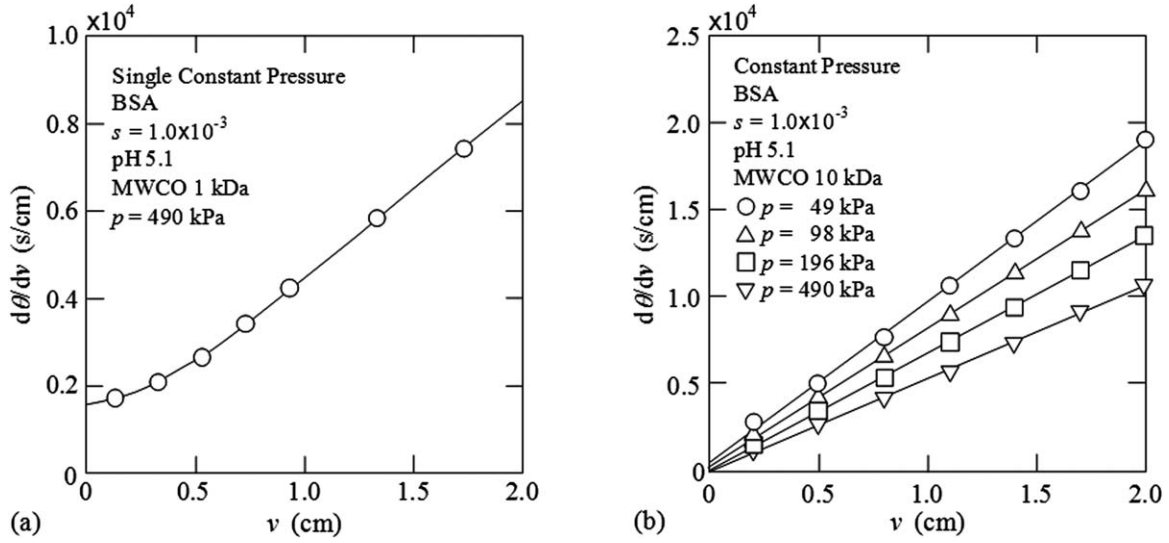

Figure 5. Flux decline behaviors for comparison to single step-up pressure filtration.

(a) Single constant pressure filtration with considerable membrane resistance, and (b) conventional constant pressure filtration with negligible membrane resistance.

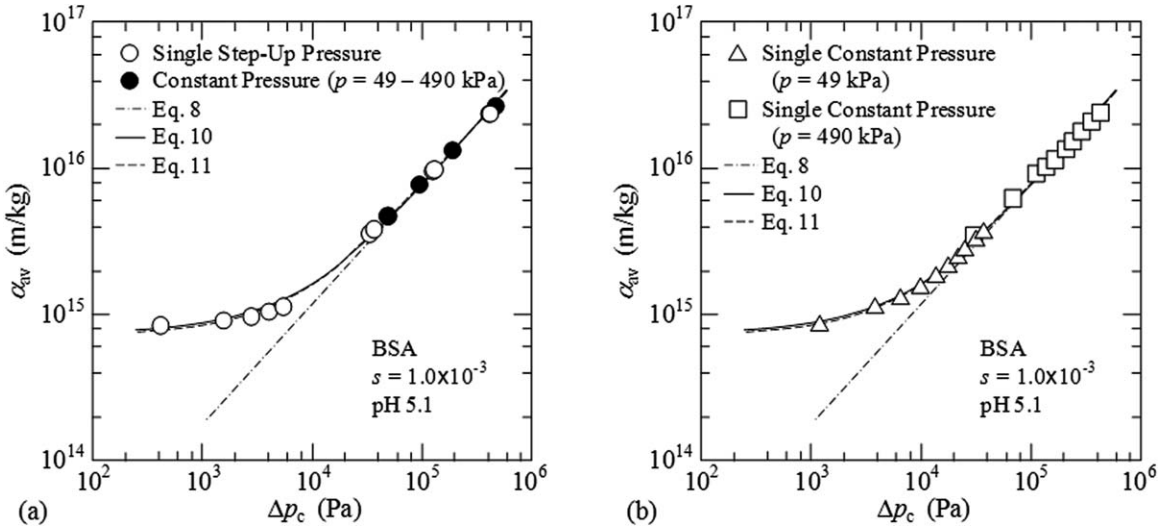

Figure 6. Pressure dependence of average specific cake resistance.

(a) Comparison between single step-up pressure filtration data and conventional constant pressure filtration data, and (b) single constant pressure filtration data.

$d\theta/dv$ vs. v shown in Figure 3a, as described previously. It is of importance to emphasize that the pressure dependence of α_{av} is available over an extremely wide pressure range from a low of 0.42 to as high as 420 kPa from only one filtration test by the method developed. The increase in α_{av} with Δp_c is gradual in the low-pressure region under approximately 6 kPa, but the plots become almost linear in accordance with Eq. 8 when Δp_c somewhat exceeds 20kPa. This suggests that there is a threshold pressure below which α_{av} approach a nearly pressure independent value, as pointed out by Tiller and Cooper.[25] This also means that the compressibility of the BSA cake depends on the range of Δp_c and that it becomes lower under the relatively low-pressure conditions. Therefore, it is expected that the filtration rate in constant pressure filtration increases in almost direct proportion to the applied pressure in the range of low pressures and that the increase in the applied pressure is not so effective in increasing filtration rate in the high-pressure range. The solid and dashed curves on Figure 6a are obtained from the curve fitting based on Eqs. 10 and 11, respectively. Both curves correspond with each other and are in very good agreement with the plots over a whole range of pressures evaluated from the single step-up pressure filtration data.

The filled circles shown in Figure 6a are the results evaluated from a series of the conventional constant pressure filtration tests conducted using the ultrafiltration membrane with the MWCO of 10 kDa at pressures of 49, 98, 196, and 490 kPa. The value of α_{av} corresponding to each pressure is determined from the slope of the straight line of $d\theta/dv$ vs. v shown in Figure 5b by use of Eq. 13. Such plots thus obtained become virtually linear in line with Eq. 8, and it is found that the value of the compressibility coefficient n_1 in Eq. 8 is around 0.76 for the filter cake of BSA, indicating high compressibility. However, it should be noted that Eq. 8 can only be used in restricted pressure ranges due to the inadequate fit of the two parameter power law expression. The plots are in good agreement with the data obtained from the single step-up pressure filtration test. This clearly demonstrates that the internal pore structure of step-up pressure filter cake is identical to that of constant pressure filter cake provided the pressure drop across the cake is the same. This also implies that equilibrium porosities are reached instantaneously with changes in pressure. However, it would be impractical to produce the data of α_{av} under extremely low pressures by the conventional constant pressure filtration tests because of experimental difficulties such as adjusting pressure. Furthermore, the tests are very tedious because several experimental runs are required in order to obtain the pressure dependence of α_{av}.

The triangles and squares depicted in Figure 6b are the results evaluated from the single constant pressure filtration tests conducted using the ultrafiltration membrane with the MWCO of 1 kDa under the pressure conditions of 49 and 490 kPa, respectively. It is very difficult to evaluate the values of α_{av} at the extremely low pressures from the test conducted at the pressure of 490 kPa. Conversely, the pressure dependence of α_{av} in the high-pressure range cannot be found from the test conducted at the pressure of 49 kPa because it is impossible to obtain the values of α_{av} in the pressure range above the applied filtration pressure. Consequently, at least two single constant pressure filtration tests in which the applied filtration pressure differ widely between both must be conducted in order to evaluate the pressure dependence of α_{av} over a wide pressure range.

To examine the deviations in the experimental data in single step-up pressure filtration tests, Figure 7 illustrates the experimental data obtained from five runs carried out under the same operating conditions. The plots of α_{av} vs. Δp_c are indicated by the logarithmic and linear scales in Figures 7a and b, respectively. The linear scale was used in order to exaggerate the deviations in the data obtained from single step-up pressure filtration tests. Data indicate that the experimental error remains within the scope of 5% above or below the solid curve fitted by Eq. 11. Therefore, our results clearly show that the single step-up pressure filtration test is a highly reproducible and effective method in evaluating the pressure dependence of α_{av} expeditiously and easily.

Effects of solution concentration and solution environments

The possible effects of solution concentration and such solution environments as pH and salt concentration are

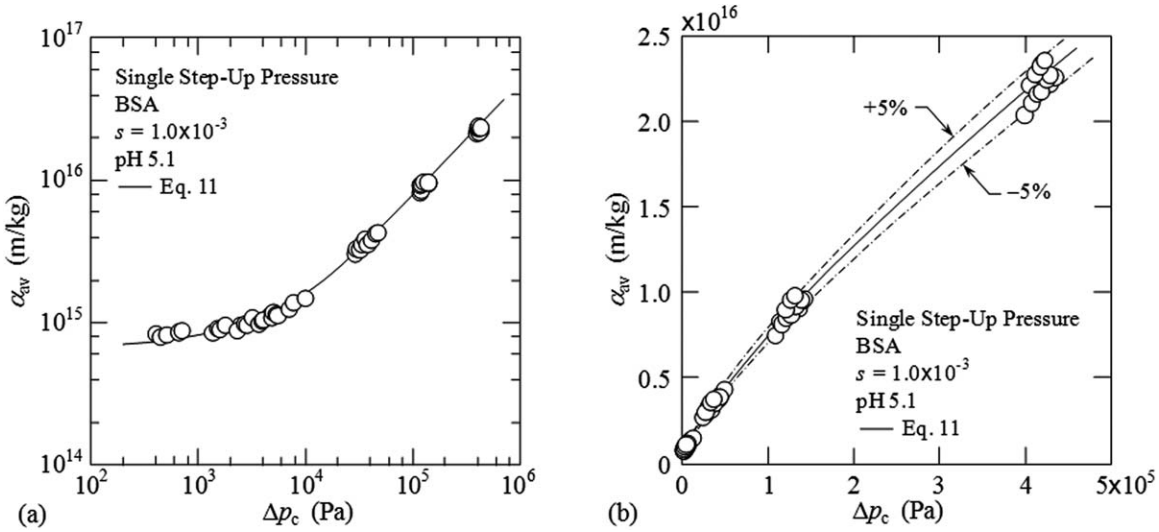

Figure 7. Reproducibility of pressure dependence of average specific cake resistance in single step-up pressure filtration test.

(a) Plots indicated by logarithmic scale, and (b) plots indicated by linear scale.

discussed here in the case of BSA solution as an example. Figure 8 shows the influence of the mass fraction s of BSA molecules in the solution on the relation between α_{av} and Δp_c. The values of s range from 1.0×10^{-3} to 5.0×10^{-3}. Our experimental data suggest that the deviations in α_{av} vs. Δp_c data between the solution concentrations are not so obvious in accord with the results obtained previously although the data obtained at the concentration of 5.0×10^{-3} exhibit slightly higher α_{av}.[13] Therefore, it is confirmed that Eq. 7 can be used in place of the rigorous Eq. 4 within the range of concentrations employed in this study.

Figure 9 shows the effect of solution environments such as pH and salt concentration on the pressure dependence of the average specific resistance α_{av} of BSA cake. Previous studies of the effect of pH on α_{av} suggested that α_{av} has a distinct maximum around the isoelectric point, i.e., the point of no net charge on the molecules.[3,20] However, the pressure dependence of α_{av} is very similar in the relatively low-pressure range below 6 kPa regardless of the solution pH. As the pressure drop Δp_c across the cake is increased, the curves for α_{av} at pH 3.5 and 7.0 lie below the curve for pH 5.1 of the isoelectric point of BSA. It should be noted that the cake porosity reflects a balance between the electrostatic repulsion force between charged BSA molecules forming the cake and the compressive pressure which tends to drive the proteins closer together.[28] In response to the increase in applied pressure, the cake is compressed and the intermolecular distance between BSA molecules in the cake becomes small. As a result, a mutual electrostatic repulsion force which acts between BSA molecules becomes more marked at pH 3.5 and 7.0 than at pH 5.1 since BSA molecules are electropositive at pH 3.5 or electronegative at pH 7.0. Therefore, the decrease in the cake porosity associated with the increase in the pressure is suppressed at pH 3.5 and 7.0 where proteins have charge, leading to a reduction in α_{av}, as discussed elsewhere.[3,29] In contrast, as the sufficient intermolecular distance is kept between BSA molecules in the cake in the range of relatively low pressure, such a charge effect is negligible, leading to the similar results at either pH values. In the figure, the results evaluated from a series of the conventional constant pressure filtration tests are shown as the filled circles and triangles for pH 5.1 and 3.1, respectively, and they are in excellent agreement with those evaluated from the single step-up pressure filtration test.

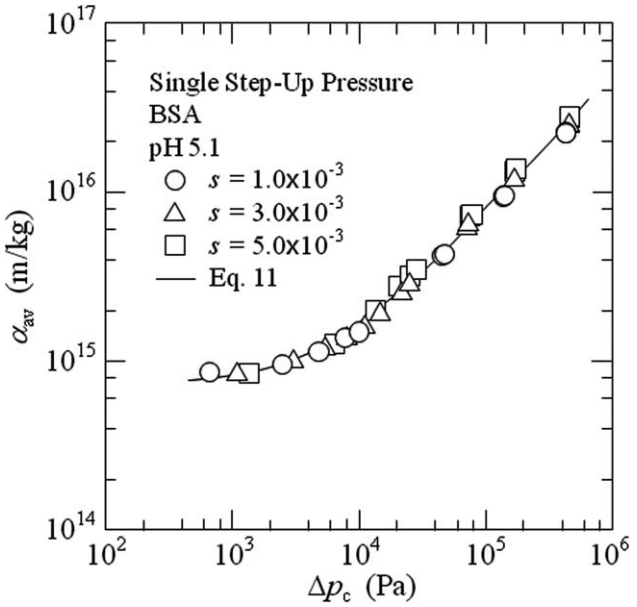

Figure 8. Effect of solution concentration on pressure dependence of average specific resistance of BSA cake.

Subsequently, in order to investigate the dependence of α_{av} on the salt concentration, the single step-up pressure filtration tests were conducted under the solution environment of pH 3.5 and the NaCl concentration C_s of 200 mol/m^3, and the results are shown in Figure 9. When the salts are added, α_{av} at pH 3.5 increases significantly and approach that at the isoelectric point without the salt addition. The salt addition leads to a less extensive diffuse double layer. Such charge-shielding between BSA molecules arising from the existence of salts would reduce electrostatic repulsion between the molecules. Thus, the difference in α_{av} at between pH 3.5 and 5.1 becomes less noticeable, and the cake is sufficiently

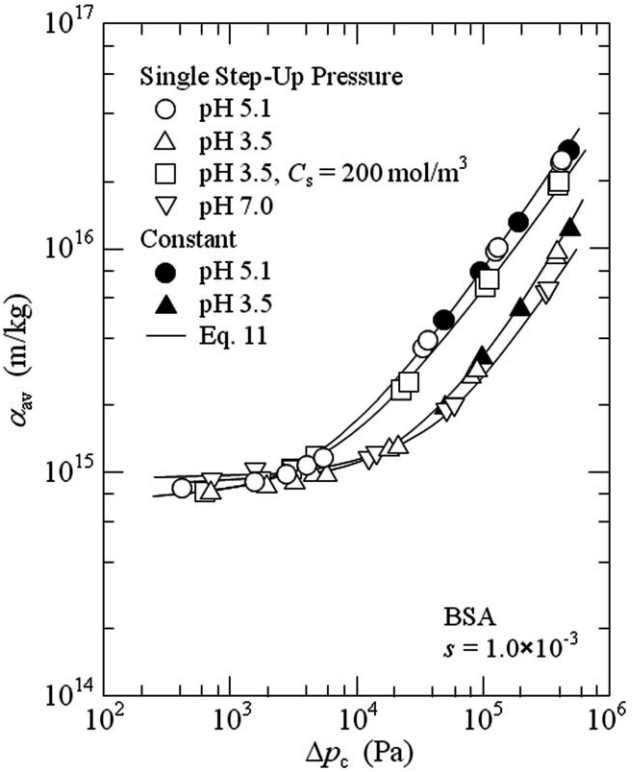

Figure 9. Effect of such solution environments as pH and salt concentration on pressure dependence of average specific resistance of BSA cake.

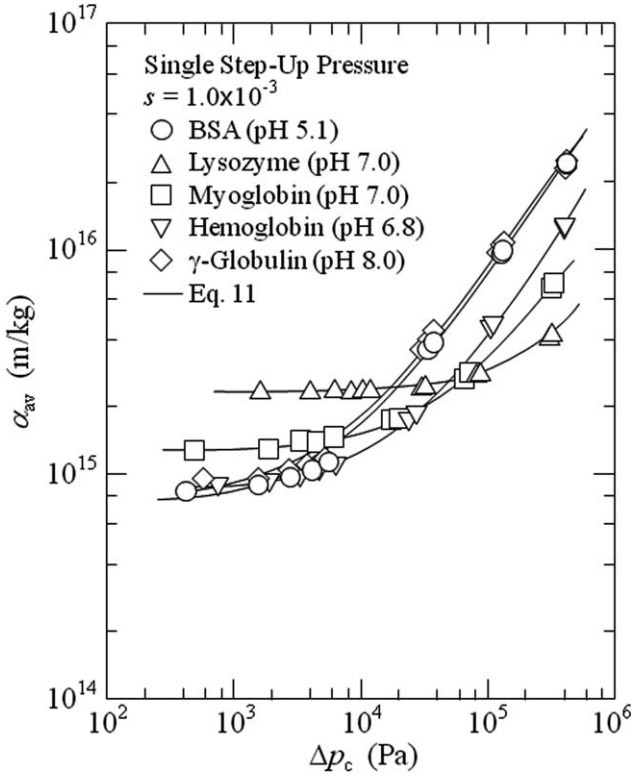

Figure 10. Pressure dependence of average specific cake resistance for various protein solutions.

compressed in the high-pressure range even at pH 3.5, leading to high specific cake resistance. These results provide important insights into the physical phenomena governing the structural changes in the filter cake comprised of BSA.

Pressure dependence of specific cake resistance of a variety of proteins and nanoparticles

The single step-up pressure filtration tests were conducted for a variety of protein solutions and nano-colloids, and the pressure dependence of α_{av} was evaluated in a relatively wide pressure range. Figure 10 illustrates the relation between α_{av} and Δp_c evaluated from the filtration tests for the protein solutions of BSA, lysozyme, myoglobin, hemoglobin, and γ-globulin. The values of the solution pH prepared are shown in the figure. In any of these protein solutions, the data can be well approximated by Eq. 11 over the entire pressure range. In either protein, α_{av} undergoes a profound change with Δp_c as Δp_c is increased. It is important to note that α_{av} decreases with increasing molecular weight of proteins with the exception of γ-globulin in the low-pressure range where the charge effect of protein molecules is negligible. However, the magnitude relationship of α_{av} becomes complicated in the high-pressure range probably under the influence of the charge and deformability of proteins.

The observed pressure dependence of α_{av} is shown in Figure 11 for nano-colloids of silica sol with the mean specific surface area sizes d_s of 4.8, 13.3, and 99.7 nm. It can be seen that the values of α_{av} increase with the decrease in the particle size over the entire range of pressures tested. In each case, Eq. 11 provides a fairly good approximation of experimental data. The slope of α_{av} vs. Δp_c curve increases as Δp_c is increased. Table 2 lists the best values of the adjustable parameters in Eqs. 9 and 11 chosen to fit

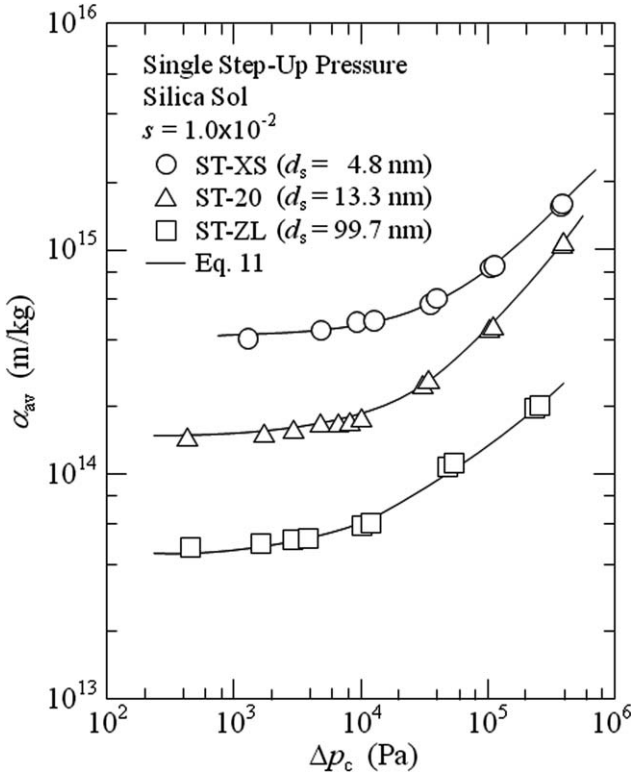

Figure 11. Pressure dependence of average specific cake resistance for silica sols with various particle sizes.

Table 2. Values of Adjustable Parameters in Eqs. 9 and 11 for a Variety of Nanocolloids

	Eq. 9			Eq.11		
Nano-Colloids	a_0 (m/kg)	P_{a1}(Pa)	n_2 (−)	a_1 (m/kg)	P_{a2}(Pa)	n_3 (−)
BSA (pH 5.1)	7.39×10^{14}	3.12×10^{3}	1.03	7.08×10^{14}	5.54×10^{3}	0.79
BSA (pH3.5)	8.79×10^{14}	4.54×10^{4}	1.28	8.78×10^{14}	4.13×10^{4}	1.03
BSA (pH3.5, C_s = 200 mol/m^3)	7.21×10^{14}	3.91×10^{3}	1.09	7.76×10^{14}	8.16×10^{3}	0.82
BSA (pH 7.0)	9.42×10^{14}	4.94×10^{4}	1.85	9.44×10^{14}	5.26×10^{4}	0.97
Lysozyme	2.34×10^{15}	4.97×10^{5}	2.45	2.34×10^{15}	4.51×10^{5}	1.12
Myoglobin	1.26×10^{15}	2.94×10^{4}	1.14	1.26×10^{15}	4.16×10^{4}	0.76
Hemoglobin	8.02×10^{14}	1.12×10^{4}	1.27	8.21×10^{14}	1.75×10^{4}	0.86
γ-Globulin	7.95×10^{14}	1.80×10^{3}	0.88	7.45×10^{14}	3.60×10^{3}	0.73
ST-XS	4.51×10^{14}	5.37×10^{4}	1.04	4.52×10^{14}	7.57×10^{4}	0.70
ST-20	1.46×10^{14}	2.40×10^{4}	1.17	1.47×10^{14}	3.54×10^{4}	0.79
ST-ZL	4.20×10^{13}	3.07×10^{3}	0.49	4.29×10^{13}	6.90×10^{3}	0.43

experimental data obtained throughout this investigation. The correlation coefficients are 0.99 for all cases, indicating that the parameters are highly correlated.

Conclusion

The single step-up pressure filtration test was conducted by filtering a variety of nanocolloids with a ultrafiltration membrane having a high hydraulic resistance, in order to find the relation between the average specific cake resistance α_{av} and the effective pressure drop Δp_c across the filter cake over a wide range of pressures. Focusing on the distinct variation of Δp_c with progression of filtration, the data of the reciprocal filtration rate ($d\theta/dv$) vs. the filtrate volume v per unit membrane area permitted us to determine the pressure dependence of α_{av} based on the compressible cake filtration theory. The single step-up pressure filtration test was able to adequately evaluate the pressure dependence of α_{av} for a wider range of pressures from extremely low pressures to high pressures from only one filtration test, unlike the conventional constant pressure filtration test and the single constant pressure filtration test. The results derived from this method were compared with the conventional constant pressure filtration data collected for a variety of filtration pressures and the single constant pressure filtration data, excellent agreement being observed. The data obtained using this method revealed the effect of the kind of protein, size of nanoparticles, the solution concentration, and the solution environment such as pH and the salt concentration on the pressure dependence of α_{av}.

Acknowledgments

This work has been partially supported by a Grant-in-Aid for Scientific Research from The Ministry of Education, Culture, Sports, Science and Technology, Japan and from The Ministry of the Environment, Japan, and by The Steel Foundation for Environmental Protection Technology. The authors wish to acknowledge with sincere gratitude the financial support leading to the publication of this article.

Notation

a_0 = empirical constant in Eq. 9, m/kg
a_1 = empirical constant in Eq. 11, m/kg
C_s = NaCl concentration in solution, mol/m^3
d_s = mean specific surface area size of nanoparticles, m
$(d\theta/dv)_m$ = reciprocal filtration rate at onset of filtration, s/m
m = ratio of mass of wet to mass of dry cake
n_1 = compressibility coefficient defined in Eq. 8
n_2 = empirical constant in Eq. 9
n_3 = empirical constant in Eq. 11
p = applied filtration pressure, Pa
p_{a1} = empirical constant in Eq. 9, Pa
p_{a2} = empirical constant in Eq. 11, Pa
p_i = some low pressure below which local specific cake resistance α is kept constant, Pa
p_L = local hydraulic pressure, Pa
p_m = liquid pressure drop across membrane, Pa
p_s = local solid compressive pressure, Pa
p_1 = applied filtration pressure at the first stage in single step-up pressure filtration, Pa
p_2 = applied filtration pressure at the second stage in single step-up pressure filtration, Pa
p_3 = applied filtration pressure at the third stage in single step-up pressure filtration, Pa
p_4 = applied filtration pressure at the fourth stage in single step-up pressure filtration, Pa
R_c = hydraulic resistance of filter cake, m^{-1}
R_m = hydraulic resistance of membrane, m^{-1}
s = mass fraction of solids in colloids
u = apparent liquid velocity relative to solids in cake at distance ω from membrane, m/s
u_1 = filtration rate, m/s
v = cumulative filtrate volume per unit membrane area, m^3/m^2

Greek letters

α = local specific cake resistance, m/kg
α_{av} = average specific cake resistance, m/kg
α_1 = empirical constant in Eq. 8, $kg^{-m_1-1}m^{1+m_1}S^{zm_1}$
Δp_c = pressure drop across filter cake, Pa
θ = filtration time, s
μ = viscosity of filtrate, Pa s
ρ = density of filtrate, kg/m^3
ρ_s = density of solids, kg/m^3
ω = net solid volume per unit membrane area lying from membrane up to an arbitrary position in filter cake, m^3/m^2
ω_0 = net solid volume of entire filter cake per unit membrane area, m^3/m^2

Literature Cited

1. Reihanian H, Robertson CR, Michaels AS. Mechanism of polarization and fouling of ultrafiltration membranes by proteins. *J Membr Sci*. 1983;16:237–258.
2. Suki A, Fane AG, Fell CJD. Flux decline in protein ultrafiltration. *J Membr Sci*. 1984;21:269–283.
3. Iritani E, Nakatsuka S, Aoki H, Murase T. Effect of solution environment on unstirred dead-end ultrafiltration charactersistics of proteinaceous solutions. *J Chem Eng Jpn*. 1991;24:177–183.
4. Nakakura H, Yamashita A, Sambuichi M, Osasa K. Electrical conductivity measurement of filter cake in dead-end ultrafiltration of protein solution. *J Chem Eng Jpn*. 1997;30:1020–1025.
5. Shirato M, Murase T, Iritani E, Tiller FM, Alciatore AF. Filtration in the chemical process industry. In: Matteson MJ, Orr C. *Filtration: Principles and Practices*. New York: Marcel Dekker, Inc.; 1987: 299–420.

6. Olivier J, Vaxelaire J, Vorobiev E. Modelling of cake filtration: an overview. *Sep Sci Technol*. 2007;42:1667–1700.
7. Tarleton ES, Wakeman RJ. Solid/Liquid Separation: Equipment Selection and Process Design. Oxford: Elsevier, Ltd.; 2007.
8. Tiller FM, Crump JR, Ville F. A revised approach to the theory of cake filtration. *Proc Intern Symp Fine Particle Process*. 1980;2: 1549–1582.
9. Leu WF, Tiller FM. Experimental study of the mechanism of constant pressure cake filtration: clogging of filter media. *Sep Sci Technol*. 1983;18:1351–1369.
10. Leu WF, Tiller FM. An overview of solid–liquid separation in coal liquefaction processes. *Powder Tecnol*. 1984;40:65–80.
11. Vorobiev E. Derivation of filtration equations incorporating the effect of pressure redistribution on the cake-medium interface: a constant pressure filtration. *Chem Eng Sci*. 2006;61:3686–3697.
12. Teoh SK, Tan RBH, Tien C. A new procedure for determining specific filter cake resistance from filtration data. *Chem Eng Sci*. 2006; 61:4957–4965.
13. Iritani E, Katagiri N, Takaishi Y, Kanetake S. Determination of pressure dependence of permeability characteristics from single constant pressure filtration test. *J Chem Eng Jpn*. 2011;44:14–23.
14. Iritani E, Katagiri N, Kanetake S. Determination of cake filtration characteristics of dilute suspension of bentonite from various filtration tests. *Sep Purif Technol*. 2012;92:143–151.
15. Murase T, Iritani E, Cho JH, Shirato M. Determination of filtration characteristics based upon filtration tests under step-up pressure conditions. *J Chem Eng Jpn*. 1989;22:373–378.
16. Iritani E, Nagaoka H, Katagiri N. Determination of filtration characteristics of yeast suspension based upon multistage reduction in cake surface area under step-up pressure conditions. *Sep Purif Technol*. 2008;63:379–385.
17. Shirato M, Aragaki T, Iritani E. Analysis of constant pressure filtration of power-law non-Newtonian fluids. *J Chem Eng Jpn*. 1980;13: 61–66.
18. Tiller FM, Shirato M. The role of porosity in filtration: VI. New definition of filtration resistance. *AIChE J*. 1964;10:61–67.
19. Tiller FM, Cooper HR. The role of porosity in filtration: IV. Constant pressure filtration. *AIChE J*. 1960;6:595–601.
20. Iritani E, Mukai Y, Hagihara E. Measurements and evaluation of concentration distributions in filter cake formed in dead-end ultrafiltration of protein solutions. *Chem Eng Sci*. 2002;37:53–62.
21. Iritani E, Hattori K, Murase T. Analysis of dead-end filtration based on ultracentrifugation method. *J Membr Sci*. 1993;81:1–13.
22. Iritani E, Katagiri N, Nakano D. Flux decline behaviors in inclined dead-end ultrafiltration of BSA solutions. *Chem Eng J*. 2012;184:98–105.
23. Tiller FM. The role of porosity in filtration, Part 3: variable-pressure-variable-rate filtration. *AIChE J*. 1958;4:170–174.
24. Sperry DR. Note and correspondence: a study of the fundamental laws of filtration using plant-scale equipment. *Ind Eng Chem*. 1921; 13:1163–1164.
25. Tiller FM, Cooper H. The role of porosity in filtration: Part V. porosity variation in filter cakes. *AIChE J*. 1962;8:445–449.
26. Tiller FM, Lue WF. Basic data fitting in filtration. *J Chinese Inst Chem Engr*. 1980;11:61–70.
27. Iritani E, Katagiri N, Sengoku T, Yoo KM, Kawasaki K, Matsuda A. Flux decline behaviors in dead-end microfiltration of activated sludge and its supernatant. *J Membr Sci*. 2007;300:36–44.
28. Opong WS, Zydney AL. Hydraulic permeability of protein layers deposited during ultrafiltration. *J Colloid Interf Sci*. 1991;142:41–60.
29. Iritani E, Hattori K, Murase T. Evaluation of dead-end ultrafiltration properties by ultracentrifugation method. *J Chem Eng Jpn*. 1994;27: 357–362.

Manuscript received Jun. 18, 2013, and revision received Sept. 10, 2013.